

Active ion transporters from readily accessible acyclic octapeptides containing 3-aminobenzoic acid and alanine†

Bahiru P. Benke and Nandita Madhavan*

Cite this: *Chem. Commun.*, 2013, **49**, 7340Received 5th June 2013,
Accepted 24th June 2013

DOI: 10.1039/c3cc44224a

www.rsc.org/chemcomm

Ion transporters have been developed from acyclic octapeptides comprising *L/D* alanine and *m*-aminobenzoic acid. These octapeptides transport cations up to 3 times faster than their cyclic analog through lipid vesicles. Preliminary CD, XRD and computational studies allude to a 6–9 Å wide tetrameric ion channel as the active ion transporter.

Transmembrane ion transporters play a key role in maintaining the cell volume, regulating ion flow across cell membranes and establishing a resting membrane potential in the body.¹ Synthetic ion transporters that mimic nature's efficient as well as selective ion conductance are attractive for use as molecular machines² and sensors.^{3–5} For *in vivo* and *in vitro* applications it is desirable to derive ion transporters from non-toxic oligopeptides. Several peptide derived ion transporters have been developed that exploit the amphiphilicity, intra- or intermolecular hydrogen bonding in peptides.^{6–12} A simplistic channel design utilizing small oligopeptides derived from alternating *D* and *L*-amino acids, similar to the highly active natural ion channel Gramicidin A,¹³ remains largely unexplored. Oligopeptides that mimic the structure and/or activity of Gramicidin have been developed by Koert^{14–16} and Inoue.^{17,18} Among the smallest and most active oligopeptide ion transporters comprising alternating *D* and *L*-amino acids are the cyclic octapeptides initially reported by Ghadiri and co-workers.^{19,20} However, the cyclization and purification of these peptides is non-trivial. Herein, we present ion transporters from acyclic octapeptides **1** and **2** containing *L* and *D* alanine and 3-aminobenzoic acid units that can be readily synthesized and transport cations even more efficiently than their cyclic analog **3** (Chart 1).

The acyclic octapeptides comprise hydrophobic residues and aromatic units in order to facilitate membrane insertion. The aromatic groups also serve as turn inducing elements and could potentially aid transmembrane ion transport similar to the tryptophan units in Gramicidin. Octapeptide **1** was synthesized starting from

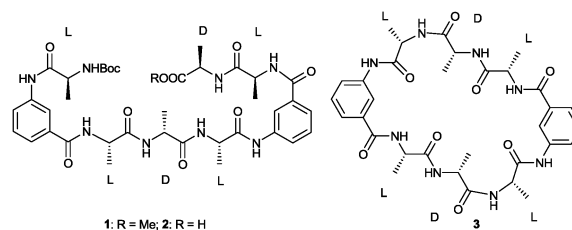
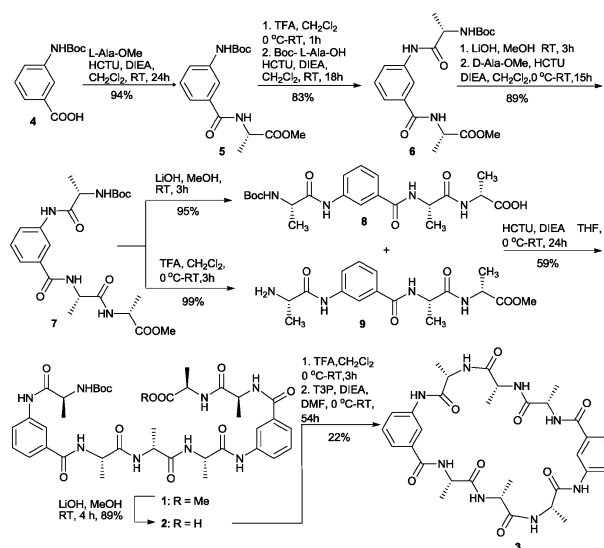


Chart 1 Octapeptide ion transporters.

m-aminobenzoic acid and *L*-alanine. Boc protected *m*-aminobenzoic acid **4** and *L*-Ala-OMe were treated with HCTU and diisopropylethylamine to form the dipeptide **5** in 94% yield (Scheme 1).²¹ Dipeptide **5** was deprotected using trifluoroacetic acid and reacted with Boc-*L*-Ala-OH to give tripeptide **6** in 83% yield. Hydrolysis of tripeptide **6** and subsequent reaction with *D*-Ala-OMe afforded tetrapeptide **7** in 89% yield. Selective deprotection of tetrapeptide **7** resulted in tetrapeptides **8** and **9**, which were coupled to give octapeptide **1** in 59% yield. Octapeptide **2** was obtained in 89% yield by hydrolyzing octapeptide **1**. Cyclic peptide **3** was synthesized to compare the ion transport



Scheme 1 Synthesis of octapeptides 1–3.

Department of Chemistry, Indian Institute of Technology Madras, Chennai – 600036, Tamil Nadu, India. E-mail: nanditam@iitm.ac.in; Fax: +91-44-22574202

† Electronic supplementary information (ESI) available: Detailed experimental procedures, characterization of compounds, analysis and fitting of fluorescence data, computational details, crystallographic data (CIF) of tetrapeptide **7** (CCDC 923387). For ESI and crystallographic data in CIF or other electronic format see DOI: 10.1039/c3cc44224a

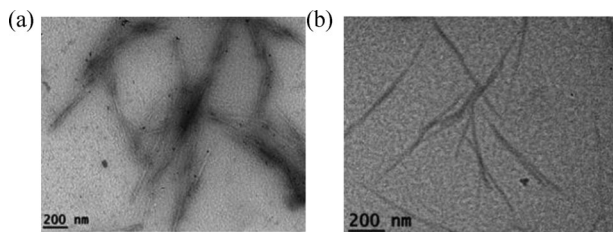


Fig. 1 TEM images of (a) cyclic peptide 3; (b) acyclic peptide 1.

efficiency of the acyclic octapeptide **1** with its cyclic analog. Peptide **3** was obtained in 22% yield by deprotecting octapeptide **1** and cyclizing the resulting peptide in the presence of T3P.

Cyclic peptides containing a single 3-amino-2-methylbenzoic unit with alternating D- and L-amino acids have been reported to form pores.²² The pore forming ability of cyclic peptides containing two 3-aminobenzoic acid units has not been experimentally determined.²³ Transmission electron microscopy (TEM) and atomic force microscopy (AFM) images of cyclic peptide **3** showed nanotube bundles similar to those obtained for the cyclic peptide containing a single aromatic unit (Fig. 1a and ESI†). The presence of an extra aromatic unit did not hamper self-assembly of **3** and gave 5–15 nm wide bundles, probably *via* the aggregation of 10–15 cyclic peptide **3** units.²² TEM images of the acyclic octapeptide **1** were similar to those obtained for the cyclic peptide **3** excluding the fact that the nanotube bundles were 10–20 nm wide. The wider nanotube bundles could be attributed to either nanotubes with bigger diameters or larger number of peptides in the aggregates (Fig. 1b).

The ion transport efficiency of octapeptide **1** was gauged using fluorescence spectroscopy.^{24,25} Lipid vesicles of ca. 100 nm diameter encapsulated by the pH sensitive 8-hydroxypyrene-1,3,6-trisulfonic acid trisodium salt (HPTS) dye were prepared for the studies *via* extrusion.²⁶ A solution of the peptide in DMSO was added to the vesicles, following which aqueous NaOH (0.5 N) was added to create a pH gradient of 0.6 units (Fig. 2a). The ion transport activity of the peptides was determined by measuring the steady increase in fluorescence intensity of the deprotonated HPTS dye upon addition of NaOH.²⁷ This increase in fluorescence is attributed to an increase in the concentration of the deprotonated dye inside vesicles due to Na⁺/OH⁻ symport or Na⁺/H⁺ antiport *via* the peptides. Finally, detergent Triton X was added to ensure equilibration of the HPTS dye. Fluorescence studies showed an increase in the concentration of deprotonated HPTS when peptides **3** and **1** were added (Fig. 2b), indicating that the peptides were transporting ions. Control experiments showed background ion transport, which was accelerated with DMSO ($k = 0.0157 \text{ s}^{-1}$). Therefore, actual transport rates through peptides were determined by fitting the curves to eqn (1),^{21,28}

$$\text{Rate} = Ae^{-k_1 t} + Be^{-k_2 t} + C \quad (1)$$

where k_1 corresponds to the peptide transport rate and k_2 corresponds to DMSO transport. The k_2 value in eqn (1) was determined by the control experiment and kept fixed while fitting the data.²¹ Acyclic peptide **1** was found to be twice as active as cyclic peptide **3** (Table 1), making it an attractive new scaffold for ion channels. However, high concentrations of peptides (27 mol%) were required to observe activity due to the large background transport. The deprotected acyclic peptide **2** containing the free carboxyl group was found to

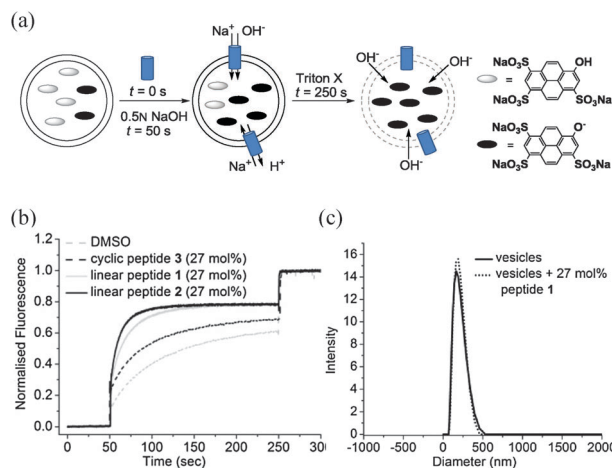


Fig. 2 (a) Schematic representation of the HPTS assay (channel mechanism); (b) change in fluorescence intensity of the deprotonated HPTS dye upon adding peptides **1–3**; (c) DLS data for vesicles with peptide **1**.

Table 1 Comparison of cation transport rates through peptides **1–3**

S. no.	Peptide	MOH	k_1^c (s ⁻¹)
1	3 ^a	NaOH	0.032 ^d
2	1 ^a	NaOH	0.064 ^d
3	1 ^a	KOH	0.067 ^d
4	1 ^a	LiOH	0.067 ^d
5	2 ^a	NaOH	0.096 ^d
6	2 ^b	NaOH	0.084 ^e
7	2 ^b	KOH	0.083 ^e
8	2 ^b	LiOH	0.084 ^e

^a 27 mol%. ^b 13.5 mol% with respect to lipid. ^c Obtained by fitting the curve to eqn (1) with Origin 8.5. ^d $k_2 = 0.0157 \text{ s}^{-1}$. ^e $k_2 = 0.02 \text{ s}^{-1}$.

be most active (3 times more active than cyclic peptide **3**). To check whether the acyclic peptides transported other cations, the counter ion for OH⁻ was varied in the experiment. Peptides **1** and **2** were found to transport a variety of alkali metal ions efficiently (entries 2–8 Table 1). Dynamic light scattering (DLS) studies were carried out on the vesicles containing peptides to rule out the possibility of the peptides acting as detergents. The DLS data showed that the vesicles retained their integrity after addition of the peptide, indicating that the peptides were not lysing the vesicles (Fig. 2c).

Circular dichroism (CD) was used to determine the solution conformation of peptide **1**. The CD spectrum showed a positive peak at 196 nm and a negative peak at 213 nm (Fig. 3a). Analysis of the spectrum indicated a majority of β -sheet character for peptide **1**.²⁹ Furthermore, the CD spectrum of acyclic peptide **1** was similar to cyclic peptide **3** which is presumed to have β -sheet character. Obtaining the solid state conformation of peptide **1** was challenging as it aggregated to form micro crystals. Hence, the crystal structure of tetrapeptide **7** was used to gain insights into the structure of peptide **1** (Fig. 3b).³⁰ The average ψ and ϕ dihedral angles of the amino acids C5 and C16 in peptide **7** are 142° and -100°, respectively, characteristic of β -sheets.²¹

Basic computational studies were carried out to gain insights into the conformation of peptide **1**. Based on the CD and the XRD data, the beta sheet dihedral angles of amino acids were used as a starting point to obtain the equilibrium geometry of peptide **1** using MMFF/AM1

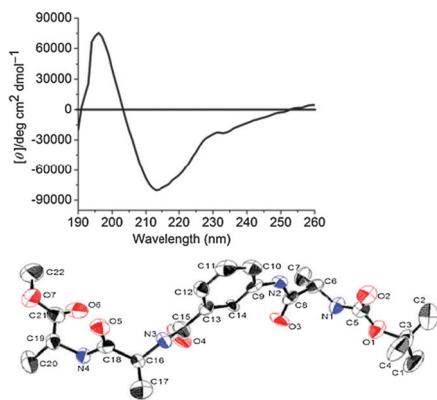


Fig. 3 (a) CD spectrum of peptide 1 (0.25 mM in methanol); (b) ORTEP diagram of tetrapeptide 7.

computations.²¹ Frequency calculations were carried out subsequently to confirm minima.³¹ Peptide 1 was found to be S-shaped (C-shaped from top), indicating that two peptides could align sideways to form a pore. Such a dimer would present the alanine methyl groups on the surface and facilitate membrane insertion as well as stabilize the channel within the membrane. The most active peptide 2 has polar carboxy groups which would presumably face the water-channel interface. Therefore, to get basic insights into the self-assembly of peptide 1, the equilibrium geometry of the laterally aligned peptide dimer having the carboxy termini on the same side was determined by AM1 calculations (Fig. 4a and b).²¹ The optimization resulted in a dimeric pore which was 6–9 Å wide and ~20 Å long. One can envision two such dimers aligning in a head to head fashion to span the lipid bilayer which has a thickness of ~40 Å (Fig. 4c). The assembly would place 8 aromatic units in the channel scaffold similar to Gramicidin A. The model explains the enhanced activity of the acyclic peptides as compared to the cyclic peptide as the self-assembly is curtailed to half of that required for the cyclic peptides.¹⁹ Such an assembly could also explain the enhanced activity of peptide 2 where all four carboxy groups would be at the peptide-water interface. The non-selective ion transport in the HPTS assay and thicker bundles seen in TEM images

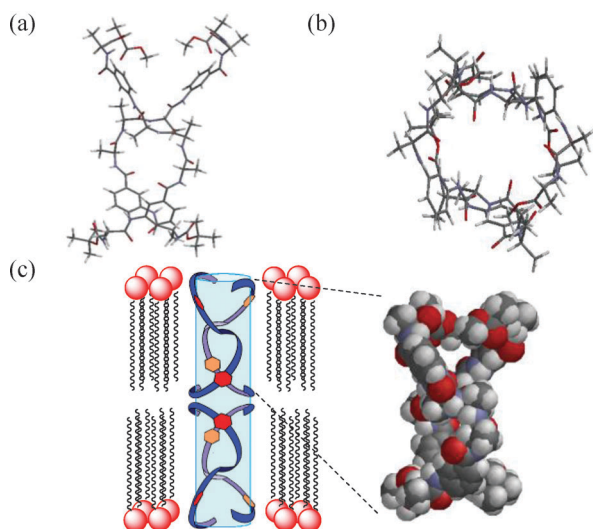


Fig. 4 Equilibrium geometry of peptide 1 dimer (a) front view; (b) top view; (c) schematic representation of the ion channel derived from peptide 1.

could also be explained by this model as the pore size is wider than that for cyclic peptides (~7 Å). However, a carrier mechanism, though unlikely cannot be ruled out.

In conclusion, a new class of readily accessible ion transporters has been derived from acyclic octapeptides containing L/D alanine and *m*-aminobenzoic acid. These peptides are more efficient than their cyclic analog in terms of synthesis and ion transport activity, making them extremely attractive for development of novel materials. CD, XRD and computational studies allude to ion mediation *via* a tetrameric pore. This model explains the higher transport activity, wider nanotube bundle formation and lower cation selectivity by the acyclic peptides as compared to their cyclic analog. Efforts are underway for enhancing and modulating ion transport through these peptides.

This research was supported by DST (SR/S1/OC-41/2009), New Delhi, India. B.P.B acknowledges CSIR, India for a research fellowship. We thank Mr V. Ramkumar for X-Ray crystallographic analysis and Dr E. Prasad for the use of his DLS instrument. We thank SAIF and the Dept. of Metallurgical and Materials Engineering I.I.T. Madras for SEM and TEM images.

Notes and references

- 1 B. Hille, *Ion Channels of Excitable Membranes*, Sinauer, Sunderland, MA, 3rd edn, 2001.
- 2 F. Xia, W. Guo, Y. Mao, X. Hou, J. Xue, H. Xia, L. Wang, Y. Song, H. Ji, Q. Ouyang, Y. Wang and L. Jiang, *J. Am. Chem. Soc.*, 2008, **130**, 8345.
- 3 Q. H. Nguyen, M. Ali, R. Neumann and W. Ensinger, *Sens. Actuators, B*, 2012, **162**, 216.
- 4 S. Hagihara, L. Gremaud, G. Bollot, J. Mareda and S. Matile, *J. Am. Chem. Soc.*, 2008, **130**, 4347.
- 5 H. Bayley and P. S. Cremer, *Nature*, 2001, **413**, 226.
- 6 P.-L. Boudreaud and N. Voyer, *Org. Biomol. Chem.*, 2007, **5**, 1459.
- 7 N. Sakai, J. Mareda and S. Matile, *Acc. Chem. Res.*, 2008, **41**, 1354.
- 8 J. K. W. Chui and T. M. Fyles, *Chem. Soc. Rev.*, 2012, **41**, 148.
- 9 G. W. Gokel and I. A. Carasel, *Chem. Soc. Rev.*, 2007, **36**, 378.
- 10 K. S. Akerfeldt, J. D. Lear, Z. R. Wasserman, L. A. Chung and W. F. DeGrado, *Acc. Chem. Res.*, 1993, **26**, 191.
- 11 R. Pajewski, R. Ferdani, J. Pajewska, N. Djedović, P. H. Schlesinger and G. W. Gokel, *Org. Biomol. Chem.*, 2005, **3**, 619.
- 12 N. Busschaert and P. A. Gale, *Angew. Chem., Int. Ed.*, 2013, **52**, 1374.
- 13 B. A. Wallace, *Prog. Biophys. Mol. Biol.*, 1992, **57**, 59.
- 14 U. Koert and J. R. Pfeifer, *Synthesis*, 2004, 1129.
- 15 U. Koert, *Phys. Chem. Chem. Phys.*, 2005, **7**, 1501.
- 16 P. Reiß, L. Al-Momani and U. Koert, *ChemBioChem*, 2008, **9**, 377.
- 17 H. Itoh, S. Matsuoka, M. Kreir and M. Inoue, *J. Am. Chem. Soc.*, 2012, **134**, 14011.
- 18 H. Itoh and M. Inoue, *Acc. Chem. Res.*, 2013, DOI: 10.1021/ar300315p.
- 19 D. T. Bong, T. D. Clark, J. R. Granja and M. R. Ghadiri, *Angew. Chem., Int. Ed.*, 2001, **40**, 988.
- 20 R. J. Brea, C. Reiriz and J. R. Granja, *Chem. Soc. Rev.*, 2010, **39**, 1448.
- 21 See ESI† for details.
- 22 R. Hourani, C. Zhang, R. van der Weegen, L. Ruiz, C. Li, S. Keten, B. A. Helms and T. Xu, *J. Am. Chem. Soc.*, 2011, **133**, 15296.
- 23 MD simulations have indicated that pore formation might be difficult.
- 24 K. Kano and J. H. Fendler, *Biochim. Biophys. Acta*, 1978, **509**, 289.
- 25 N. R. Clement and J. M. Gould, *Biochemistry*, 1981, **20**, 1534.
- 26 <http://www.avantilipids.com/>.
- 27 The steady increase in fluorescence is preceded by an initial rapid increase due to deprotonation of the dye on the external vesicle surface.
- 28 N. Madhavan, E. C. Robert and M. S. Gin, *Angew. Chem., Int. Ed.*, 2005, **44**, 7584.
- 29 Deconvoluted using the CDNN 2.1 software.
- 30 The structure was solved in the space group *P21* with an *R* factor of 8.36%. The unit cell parameters are *a* = 12.639 (2)', *b* = 10.4737(16)', *c* = 18.814(3) Å and β = 90.117(1). *Z* = 2', *V* = 2490.54(68) Å³. CCDC 923387 contains crystallographic data for peptide 7.
- 31 Geometry optimization was done using the PC SPARTAN PRO Semi-empirical program 6.0.6.